# Model of Continuous Dispersive Flow with Interactive Deadwater and Application to Gas-Phase Flow in Rotary Calciners

A continuous flow model is developed which describes flow through a vessel in which the fluid undergoes axial dispersed plug flow and some of the fluid is held back in a deadwater zone. The first three moments of the concentration-time curve are related to the three parameters of the model, and an equation is presented to predict the outlet concentration from the vessel as a function of time for an impulse input. The model is used to analyze experimental gas-phase residence-time distribution (RTD) data collected from a small rotary calciner operated at room temperature. These data are well represented by the model.

**B. B. SPENCER and M. E. WHATLEY**

Fuel Recycle Division
Oak Ridge National Laboratory‡
Oak Ridge, TN 37830

and

**J. S. WATSON**

Chemical Technology Division
Oak Ridge National Laboratory
Oak Ridge, TN 37830
and
Department of Chemical Engineering
The University of Tennessee
Knoxville, TN 37916

## SCOPE

A continuous dispersive flow model with an interactive deadwater region presently appears to be useful in analyzing several types of continuous flow equipment. Previously, such analysis has been performed using tanks-in-series with deadwater zones; the mathematics of which have been developed by Levich et al. (1967). One item that could be analyzed with the continuous model is a rotary calciner whose function is to contact a solid reactant with a gaseous reactant. Obviously, because of the internal mixing vanes and the tumbling solids, the gas will be in mixed flow. The magnitude of the axial dispersion affects the positional concentration of the gaseous reactant and hence the length of reactor required for a given mean conversion. Further, in many cases, the reaction takes place primarily in the solids bed where the gaseous reactant is trapped and released from the void spaces in the bed. It can be expected that the rate of exchange of reactant between the bed and the bulk gas phase may be significant in determining conversion. Both of these effects become more significant if the gas flow rate is low (which may be a requirement if the effluent gases from the unit are noxious and must be treated). The results of isothermal RTD experiments can be used to quantify the exchange effect even in a case where thermal convection dominates the mixing of the bulk gas phase. There are no data in the literature describing gas phase RTD in rotary calciners.

## CONCLUSIONS AND SIGNIFICANCE

The mathematics of an axial dispersion model with an interactive deadwater fraction have been developed. Gas-phase RTDs measured in a rotary calciner have been well represented by the model. However, use of the model is not restricted to the analysis of this system; it can be used to analyze data from other continuous flow systems in which a stagnant region is suspected to be present (e.g., spreading of concentration bands in packed beds).

Gas-phase RTD experiments have been performed using a rotary calciner with a 0.165-m inside diameter and a 2.17-m-long retort tube operated isothermally at room temperature. Drum rotational speeds were varied from 2.0 to 7.0 rpm, air flow rates through the drum varied from $0.097 \times 10^{-3}$ to $1.196 \times 10^{-3}$ m$^3$/s, and settled solid contents of 0.0, 5.1, and 15.3% of drum volume were featured. The model, used to analyze the data, was reduced to a two-parameter model by assuming that the deadwater fraction, $\alpha$, was calculable from the settled solids volume and porosity. The dispersion number, $\mathcal{D}$, and the interchange factor, $K$, were then computed from the moments of the experimental data. Values of $\mathcal{D}$ ranged from 0.0161 to 0.0680, and values of $K$ ranged from 0.0454 to 2.6201.

Although there is some scatter in the dispersion numbers and interchange factors presented, these data represent the best available information on gas dispersion in rotary calciners. The

Correspondence concerning this paper should be addressed to Barry B. Spencer, Oak Ridge National Laboratory, P.O. Box X, Building 7601, Oak Ridge, TN 37830.

0001-1541-83-6754-0460-$2.00 

principal limitation on the dispersion number data results from the isothermal conditions used in these experiments; most rotary calciners operate with significant thermal gradients. The exchange factors may be less dependent upon temperature fields. Scatter in the data can be partially explained by the sensitivity of the model to errors in the instrument zero line. Additionally, the assumption that the deadwater fraction can be calculated solely from the porosity of the settled solids may introduce some error since the solids may be partially fluidized by drum rotation. In the range of deadwater fractions imposed (a maximum of 8.1%), $K$ does not appreciably affect the concentration-time curves; therefore, $K$ is not known precisely.

## DEVELOPMENT OF MODEL

### Derivation of Differential and Boundary Conditions

The model is developed from a differential element of a tube where fluid enters and leaves by both bulk flow and dispersion, Figure 1. Further, the model assumes that within the element there exists a "deadwater" region occupying some fraction, $\alpha$, of the tube and a region of unobstructed flow occupying the remainder of the tube. The deadwater region consists of the gas retained within the region of the tube occupied by solid granules. These two regions exchange matter across the interface between the gas and solids bed at a net rate proportional to the difference of the concentrations in the two regions. The unsteady state material balance over each region has been shown to yield two simultaneous partial differential equations of a form previously analyzed by Van Deemter et al. (1956). These equations, the appropriate closed vessel boundary conditions and Danckwerts' (1953) initial conditions may be written in dimensionless form as follows:

$$\frac{\partial C}{\partial \theta} = \mathcal{D}\frac{\partial^2 C}{\partial z^2} - \frac{1}{(1-\alpha)}\frac{\partial C}{\partial z} - \frac{K}{(1-\alpha)}(C - C_d), \quad (1)$$

$$\frac{\partial C_d}{\partial \theta} = \frac{K}{\alpha}(C - C_d), \quad (2)$$

$$\theta = 0,\ C = 0 \text{ and } C_d = 0, \quad (3)$$

$$z = 0^+,\ (1-\alpha)\mathcal{D}\frac{\partial C}{\partial z} = C - C_{\text{in}}, \quad (4)$$

$$z = 1,\ \frac{\partial C}{\partial z} = 0, \quad (5)$$

where

$$\mathcal{D} = \frac{D}{\bar{u}L}, \quad (6)$$

and

$$K = \frac{kaL}{V}. \quad (7)$$

The above boundary conditions reduce to the boundary conditions derived by Wehner and Wilhelm (1956) for the ordinary dispersion model when $\alpha = 0$.

### Relation of the Moments of Concentration-Time Curve to Model Parameters

As Van der Laan (1957) first showed, the moments of the concentration-time curve for the dispersion model are simply related to the transfer function (i.e., Laplace transforms) of the defining differential equations. The transfer function relating the outlet concentration with dimensionless time for the present model is obtained from Eqs. 1 through 5 and may be written

$$U = \frac{4E}{(1+E)^2 e^{(1-E)/2\mathcal{D}(1-\alpha)} - (1-E)^2 e^{-(1+E)/2\mathcal{D}(1-\alpha)}}, \quad (8)$$

where

$$E = \sqrt{1 + \frac{4\mathcal{D}(1-\alpha)(\alpha s^2 - \alpha^2 s^2 + Ks)}{(\alpha s + K)}}. \quad (9)$$

See Spencer (1981a) for details. The equations used to compute the first three moments from the transfer function are given by Wen and Fan (1975). Applying those equations to Eq. 8 yields the normalized moments:

$$\bar{\theta} = 1, \quad (10)$$

$$\sigma_\theta^2 = 2\mathcal{D}(1-\alpha) - 2\mathcal{D}^2(1-\alpha)^2 \times [1 - e^{-[1/\mathcal{D}(1-\alpha)]}] + \frac{2\alpha^2}{K}, \quad (11)$$

and

$$\gamma_\theta^3 = 24\mathcal{D}^3(1-\alpha)^3\left[\left(\frac{1}{2\mathcal{D}(1-\alpha)} - 1\right) + \left(\frac{1}{2\mathcal{D}(1-\alpha)} + 1\right)e^{-[1/\mathcal{D}(1-\alpha)]}\right] + \frac{24\alpha^2\mathcal{D}^2(1-\alpha)^2}{K} \times \left[\frac{1}{2\mathcal{D}(1-\alpha)} + \tfrac{1}{2}(e^{-[1/\mathcal{D}(1-\alpha)]} - 1)\right] + \frac{6\alpha^3}{K^2} \quad (12)$$

When $\alpha = 0$, Eqs. 11 and 12 reduce to the moments of the ordinary dispersion model. If $K = 0$ it is necessary to return to the transfer function and modify the transfer function for $K = 0$. This is because the transfer function is a function of two variables ($s$ and $K$) and, therefore, the order with which the limits are taken is important. From the analysis for this special limiting case, $\bar{\theta} = (1-\alpha)$ and $\sigma_\theta^2$ and $\gamma_\theta^3$ are the same as the values given by Eqs. 11 and 12 except the terms involving $K$ are not present. Or, put another way, the results in this limiting case are the same as for the ordinary dispersion model in which the vessel size has been modified by a factor of $(1-\alpha)$. In the general case, the new model shows that the mean time is independent of the deadwater fraction and the interchange factor, however small.

With actual data one can calculate values of $\sigma_\theta^2$ and $\gamma_\theta^3$. Equations 11 and 12 are not sufficient to solve for $\mathcal{D}$, $K$ and $\alpha$ simultaneously. However, if one of the three parameters can be set, the other two can then be calculated. The equation for the fourth moment could be derived, and that would give a third equation with which to compute all three parameters. However, because small errors in the data would be magnified, particularly at large values of time, this approach does not appear to be practical for determining values of the three parameters.

### Solution to Differential Equations

Inverse transformation of Eq. 8 into the time domain will give the outlet concentration as a function of dimensionless time, $\theta$, for an impulse input. The complex inversion integral and theory of residues discussed by Mickley et al. (1957) and Wylie (1975) are

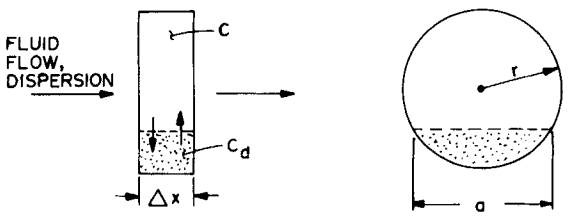


Figure 1. Differential element considered for material balance.

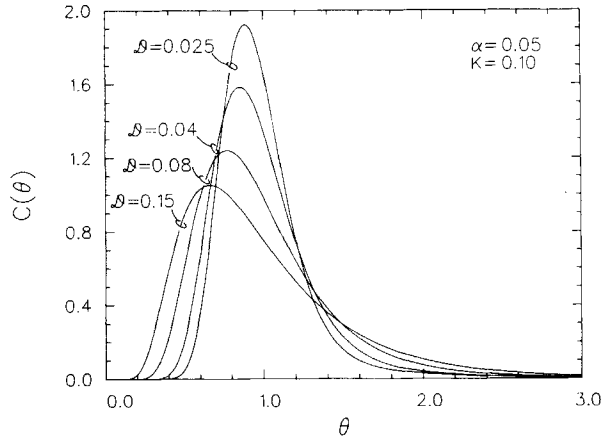


**Figure 2. Effect of varying dispersion number.**

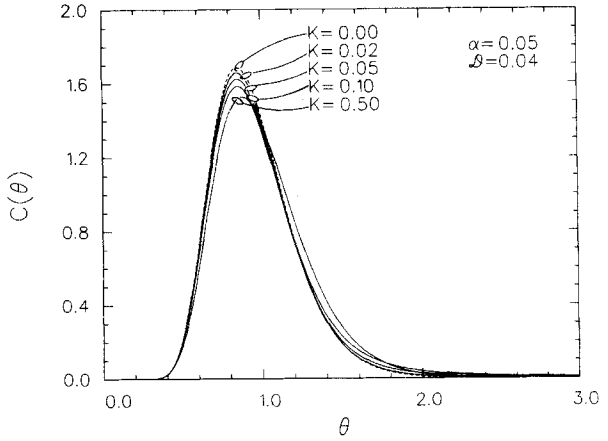


**Figure 3. Effect of varying interchange factor.**

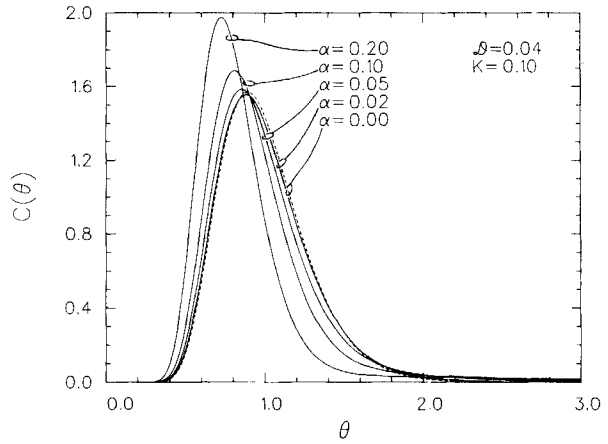


**Figure 4. Effect of varying deadwater fraction.**

often used to back transform from the Laplace domain. With no simplifying assumptions, the solution, given by Spencer (1981b), is

$$C(\theta) = \sum_{n=1}^{\infty} \frac{2\epsilon_n \left[\frac{1}{2\mathcal{D}(1-\alpha)} \sin \epsilon_n + \epsilon_n \cos \epsilon_n\right] e^{1/2\mathcal{D}(1-\alpha) + S_n^+ \theta}}{\Omega_n^+ \left[\frac{1}{4\mathcal{D}^2(1-\alpha)^2} + \frac{1}{\mathcal{D}(1-\alpha)} + \epsilon_n^2\right]}$$

$$+ \sum_{n=1}^{\infty} \frac{2\epsilon_n \left[\frac{1}{2\mathcal{D}(1-\alpha)} \sin \epsilon_n + \epsilon_n \cos \epsilon_n\right] e^{1/2\mathcal{D}(1-\alpha) + S_n^- \theta}}{\Omega_n^- \left[\frac{1}{4\mathcal{D}^2(1-\alpha)^2} + \frac{1}{\mathcal{D}(1-\alpha)} + \epsilon_n^2\right]}, \quad (13)$$

where

$$S_n^+ = \frac{1}{2(1-\alpha)}\left[\left(\phi_n - \frac{K}{\alpha}\right) + \left(\phi_n + \frac{K}{\alpha}\right)\sqrt{1 - \frac{4\alpha^2\phi_n K}{(\alpha\phi_n + K)^2}}\right], \quad (14)$$

$$S_n^- = \frac{1}{2(1-\alpha)}\left[\left(\phi_n - \frac{K}{\alpha}\right) - \left(\phi_n + \frac{K}{\alpha}\right)\sqrt{1 - \frac{4\alpha^2\phi_n K}{(\alpha\phi_n + K)^2}}\right], \quad (15)$$

$$\Omega_n^+ = 1 - \frac{\alpha^2 S_n^+(\alpha S_n^+ + 2K)}{(\alpha S_n^+ + K)^2}, \quad (16)$$

$$\Omega_n^- = 1 - \frac{\alpha^2 S_n^-(\alpha S_n^- + 2K)}{(\alpha S_n^- + K)^2}, \quad (17)$$

$$\phi_n = \frac{-4\mathcal{D}^2(1-\alpha)^2\epsilon_n^2 - 1}{4\mathcal{D}(1-\alpha)}, \quad (18)$$

and $\epsilon_n$ is given implicitly by

$$\cot \epsilon = \frac{1}{2}\left[2\mathcal{D}(1-\alpha)\epsilon - \frac{1}{2\mathcal{D}(1-\alpha)\epsilon}\right]. \quad (19)$$

The notation $\epsilon_n$ is used since there are infinitely many values of $\epsilon$ for which Eq. 19 is valid. Although the solution appears complicated, values of $C(\theta)$ can be calculated rapidly on modern digital computers. The first series in the solution converges rapidly, particularly at large values of $\theta$, and the second series converges less rapidly. Both series will always converge for $\theta > 0$. However, numerical difficulties arise in which the difference of large numbers must be calculated when $\mathcal{D}(1-\alpha)$ is less than approximately 0.02.

The first series generates a curve that is responsible for the bell shaped portion of the concentration-time curve, whereas the second series generates the slowly decaying tail. However, the results from each series cannot be decoupled and examined separately because one series may generate a negative number and the other a positive number in such a way that the sum is a real, positive value of concentration. Figures 2 through 4 show the individual effects of varying $\alpha$, $\mathcal{D}$, and $K$ while the two parameters not being varied are held constant. An increasing dispersion number, $\mathcal{D}$, has the expected effect of causing the curve to be skewed to the left, of making the peak lower and the width greater with a long tail. As the interchange factor, $K$, increases, the curve is skewed some to the right, the peak becomes lower, and the tail decays rapidly. At small values of $K$, the tail decays rather slowly. The sensitivity of the model to $K$ is embodied in the tail of the distribution rather than in the peak. Figure 3 shows that the relative differences between the curves are small (e.g., percent change) at the peak, and, even though the values of concentration are small in the tail, the relative differences between the curves are very large. The effect of an increasing deadwater fraction, $\alpha$, is to skew the curve to the left, make the peak higher and narrower, and cause the tail to decay very slowly at a set value of $K$. These plots show that considerable adjustment in the shape of the curve can be obtained, depending on the values of the parameters.

The solution can aid in determination of the model parameters. Suppose all three parameters, $\alpha$, $\mathcal{D}$, and $K$ must be determined from experimental concentration-time data (i.e., there is no independent way to determine one of the parameters). Values of $\alpha$ can be selected (a good choice since $\alpha$ must be bounded between zero and unity) and $\mathcal{D}$ and $K$ computed from Eqs. 11 and 12. The concentration-time curves can then be computed and compared with the data. The sum of squares of errors between experimental data and computed results can be used as an index to update values of $\alpha$ until a satisfactory fit is obtained.

### Comparison with Previous Models

The previous model that corresponds most closely with the model developed in the preceding section is the tanks-in-series model with

interactive deadwater developed by Levich et al. (1967). In that model, net flow through the deadwater zone corresponds to a net interchange in the present model, or

$$p(C - C_d) = ka\Delta x(C - C_d). \tag{20}$$

Assuming that $\Delta x$ is approximated by $L/N$,

$$p(C - C_d) = \frac{kaL}{N}(C - C_d). \tag{21}$$

Divide through by $(C - C_d)$, use Eq. 7 to introduce $K$, and rearrange to obtain

$$N\frac{p}{V} = K. \tag{22}$$

The correspondence between $\mathcal{D}$ and $N$ can be visualized by comparing the second moments or variances of the two models. Levich et al. (1967) calculated the first two moments for their model. These are shown below in dimensionless form:

$$\bar{\theta} = 1, \tag{23}$$

and

$$\sigma_\theta^2 = \frac{1}{N} + \frac{2\alpha^2}{N(p/V)}. \tag{24}$$

Comparing Eqs. 11 and 24, and using Eq. 22 to remove parts involving $K$, obtain

$$\frac{1}{N} = 2\mathcal{D}(1 - \alpha) - 2\mathcal{D}^2(1 - \alpha)^2\left[1 - e^{-[1/\mathcal{D}(1-\alpha)]}\right]. \tag{25}$$

If $\mathcal{D}$ is small, then

$$\frac{1}{N} \cong 2\mathcal{D}(1 - \alpha). \tag{26}$$

Thus, Eqs. 22 and 26 can be used as a basis for comparing the parameters of the two models. Of course, $\alpha$ is the same in each model. (Henceforth, denote $K$ and $\mathcal{D}$ calculated by Eqs. 22 and 26, respectively, as $K_e$ and $\mathcal{D}_e$, equivalency parameters.) If it is desired to compare numerical values of the parameters computed from the moments of the two models, then a third moment for the tanks-in-series with deadwater model is required. It is calculated to be

$$\gamma_\theta^3 = \frac{2}{N^2} + \frac{6\alpha^3}{N^2(p/V)^2} + \frac{6\alpha^2}{N^2(p/V)}. \tag{27}$$

Levich et al. (1967) were able to obtain inverse transforms of the transfer function for their model, after making several simplifications, to obtain expressions giving effluent concentration as a function of time. Different equations were developed depending upon whether $\theta$ was less than or greater than $1 - \alpha$. The solutions are discontinuous at $\theta = 1 - \alpha$. It was suggested that the three parameters, $N$, $\alpha$, and $p/V$, be estimated from the variances, maximum of the peak, and a fit of the tail of the distribution to an exponentially decaying function.

## EXPERIMENTAL APPARATUS AND PROCEDURES

Measured RTD's of the gas phase in a rotary calciner are required data for this study. A flowsheet of the experimental equipment is shown in Figure 5. The rotary calciner is an experimental Bartlett-Snow unit which has a 0.165-m inside diameter and a 2.17-m-long retort tube. Six equally-spaced mixing flights, each 2.54 cm in height and 0.64 cm in width, are attached internally over the length of the calciners drum. The unit has an electric clamshell furnace and a water cooled zone, but the data were collected at room temperature and these were not used. The calciner drum can be rotated at speeds of 2 to 8 rpm with the variable speed drive motor.

Air is metered to the calciner through two parallel rotameters. One rotameter carries the main air flow to the calciner through a diverging diffuser, which ensures that injected helium tracer fills the entire cross section upon entering the drum. The other rotameter feeds a small quantity of air to the breeching section associated with the gas entrance end of the drum. This air flows through any small gaps that exist between the stationary diverger and the rotating entrance to the drum. The back pressure, thus imposed, keeps any tracer from backmixing into the breeching section and subsequently bleeding back into the drum causing the concentration-time curves to have long tails. It is desired that long tails indicate the entrapment-release mechanism of interest to this study and not be a product of entrance deadspace. Ordinarily, the function of the breeching section is to seal the drum against the atmosphere with a grease seal and still allow solids to exit the drum. Total flow rate through the calciner is the sum of the flows through the two rotameters.

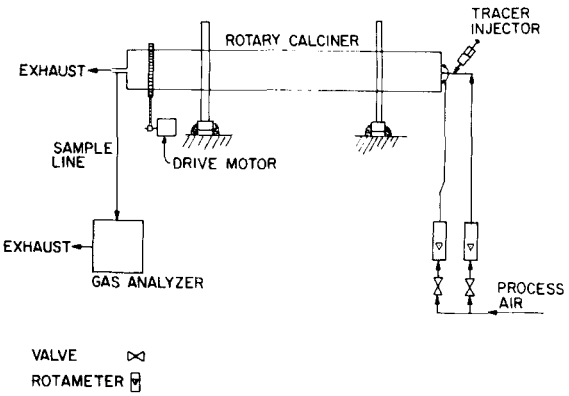


**Figure 5. Flowsheet of RTD measurement apparatus.**

The gas stream exits the calciner through a small tube (approximately 2.54 cm I.D.) and is exhausted to the atmosphere. A small quantity of sample is continuously withdrawn from the exhaust tube and analyzed using a Varian Model 936-70 helium leak detector operated in the "sniffer" mode. Mass spectrometry is the principle of operation, enabling fast response and high sensitivity. Only 5 to 10 mL of helium tracer is required for full-scale readings, depending on air flow rates. The total lag time due to the interval required for the sample to travel through the sample line plus instrument response time was measured experimentally to be 1.71 s. The lag time for the main air flow to travel from the tracer injection point through the small inlet line into the drum and later out of the drum through the exhaust tube to the sampling point was calculated from the flow rates and the volume of these two lines (429 mL). Analog output from the leak detector was recorded on strip charts providing concentration-time data after tracer injection.

Quartz sand was used as an inert solid material to simulate solid feed. The drum was set horizontal so that the inventory of solids were constant along the axial length. A measured charge of sand was placed in the drum and then the gas lines were connected, causing the solids to be captive. This prevents axial dispersion of gas due to trapped gas being carried along with solid flow. The sand used in the experiments had an average particle size of 780 $\mu$ and a void fraction of 48.9%.

Each end of the drum was constrained, as described above, so that plug flow prevailed before the gas entered and after it left the drum. Therefore, dispersive mixing of the gas occurred only inside the calciner, and the experiment qualified for analysis by closed vessel models.

## RESULTS AND DISCUSSION OF RESULTS

With the experimental apparatus described in the previous section, 71 runs were performed in which the following three parameters were varied: (1) rotational speed, (2) fraction of calciner loaded with solid or simply holdup, and (3) air flow rate. The data were analyzed by four models: (1) open vessel dispersion model, (2) closed vessel dispersion model, (3) tanks-in-series with interacting deadwater model, and (4) the new closed vessel model for

TABLE 1. EXPERIMENTAL CONDITIONS AND CALCULATED RESULTS

| 0.0% Solids Holdup | | | 5.1% Solids Holdup[a] | | | | | 15.3% Solids Holdup[b] | | | | |
|---|---|---|---|---|---|---|---|---|---|---|---|---|
| | Flow Rate | Closed | | Flow Rate | Closed | New Model | | | Flow Rate | Closed | New Model | |
| RPM | $V \times 10^3$ ($m^3/s$) | Vessel $\mathcal{D}$ | RPM | $V \times 10^3$ ($m^3/s$) | Vessel $\mathcal{D}$ | $\mathcal{D}$ | $K$ | RPM | $V \times 10^3$ ($m^3/s$) | Vessel $\mathcal{D}$ | $\mathcal{D}$ | $K$ |
| 7.0 | 0.114 | 0.0214 | 2.0 | 0.112 | 0.0475 | 0.0475 | 0.5948[c] | 2.0 | 0.100 | 0.0330 | 0.0330 | 2.6201[c] |
| 7.0 | 0.246 | 0.0246 | 2.0 | 0.238 | 0.0285 | 0.0264 | 0.2489 | 2.0 | 0.206 | 0.0236 | 0.0170 | 0.8481 |
| 7.0 | 0.490 | 0.0301 | 2.0 | 0.476 | 0.0307 | 0.0261 | 0.1315 | 2.0 | 0.423 | 0.0366 | 0.0162 | 0.3186 |
| 7.0 | 0.490 | 0.0282 | 2.0 | 0.821 | 0.0601 | 0.0491 | 0.0596 | 2.0 | 0.735 | 0.0512 | 0.0283 | 0.2827 |
| 7.0 | 0.802 | 0.0427 | 2.0 | 1.156 | 0.0832 | 0.0680 | 0.0454 | 2.0 | 1.012 | 0.0624 | 0.0430 | 0.3194 |
| 7.0 | 1.188 | 0.0674 | 3.0 | 1.156 | 0.0651 | 0.0524 | 0.0527 | 2.0 | 1.012 | 0.0549 | 0.0380 | 0.3605 |
| 5.0 | 1.188 | 0.0841 | 3.0 | 0.824 | 0.0450 | 0.0350 | 0.0652 | 3.0 | 1.014 | 0.0515 | 0.0344 | 0.3605 |
| 5.0 | 0.802 | 0.0532 | 3.0 | 0.478 | 0.0316 | 0.0255 | 0.1037 | 3.0 | 0.736 | 0.0393 | 0.0261 | 0.4578 |
| 5.0 | 0.491 | 0.0356 | 3.0 | 0.239 | 0.0314 | 0.0281 | 0.1738 | 3.0 | 0.424 | 0.0275 | 0.0185 | 0.6600 |
| 5.0 | 0.246 | 0.0255 | 3.0 | 0.112 | 0.0542 | 0.0542 | 0.5285[c] | 3.0 | 0.207 | 0.0299 | 0.0181 | 0.5215 |
| 5.0 | 0.114 | 0.0217 | 5.0 | 0.112 | 0.0620 | 0.0576 | 0.1263 | 3.0 | 0.101 | 0.0418 | 0.0384 | 1.0884 |
| 3.0 | 0.115 | 0.0248 | 5.0 | 0.239 | 0.0312 | 0.0289 | 0.2305 | 5.0 | 0.101 | 0.0559 | 0.0480 | 0.6228 |
| 3.0 | 0.246 | 0.0310 | 5.0 | 0.478 | 0.0243 | 0.0207 | 0.1687 | 5.0 | 0.207 | 0.0418 | 0.0224 | 0.3303 |
| 3.0 | 0.492 | 0.0452 | 5.0 | 0.825 | 0.0368 | 0.0301 | 0.0942 | 5.0 | 0.424 | 0.0230 | 0.0161 | 0.8335 |
| 3.0 | 0.805 | 0.0657 | 5.0 | 1.160 | 0.0512 | 0.0426 | 0.0748 | 5.0 | 0.737 | 0.0324 | 0.0209 | 0.5237 |
| 3.0 | 1.192 | 0.0738 | 7.0 | 1.149 | 0.0497 | 0.0408 | 0.0716 | 5.0 | 0.737 | 0.0405 | 0.0268 | 0.4430 |
| 2.0 | 1.196 | 0.0928 | 7.0 | 1.149 | 0.0454 | 0.0379 | 0.0842 | 5.0 | 0.424 | 0.0205 | 0.0164 | 1.2612 |
| 2.0 | 0.807 | 0.0677 | 7.0 | 0.816 | 0.0364 | 0.0297 | 0.0938 | 5.0 | 1.014 | 0.0484 | 0.0334 | 0.4031 |
| 2.0 | 0.494 | 0.0459 | 7.0 | 0.473 | 0.0252 | 0.0214 | 0.1609 | 5.0 | 0.981 | 0.0460 | 0.0310 | 0.4067 |
| 2.0 | 0.247 | 0.0316 | 7.0 | 0.237 | 0.0320 | 0.0294 | 0.2104 | 7.0 | 0.981 | 0.0485 | 0.0311 | 0.3591 |
| 2.0 | 0.115 | 0.0362 | 7.0 | 0.111 | 0.0716 | 0.0651 | 0.0924 | 7.0 | 0.981 | 0.0469 | 0.0303 | 0.3732 |
| | | | 2.0 | 0.111 | 0.0511 | 0.0511 | 0.5569[c] | 7.0 | 0.712 | 0.0352 | 0.0213 | 0.4438 |
| | | | 2.0 | 0.237 | 0.0279 | 0.0279 | 0.9701[c] | 7.0 | 0.410 | 0.0235 | 0.0213 | 1.7606 |
| | | | 2.0 | 0.474 | 0.0302 | 0.0262 | 0.1463 | 7.0 | 0.200 | 0.0364 | 0.0364 | 2.3952[c] |
| | | | 2.0 | 0.817 | 0.0514 | 0.0436 | 0.0814 | 7.0 | 0.097 | 0.0678 | 0.0678 | 1.3740[c] |

[a] Corresponds to $\alpha = 0.026$.
[b] Corresponds to $\alpha = 0.081$.
[c] Values for $\mathcal{D}$ and $K$ estimated.

dispersion with interacting deadwater. The first two models are one-parameter models, whereas the last two are three-parameter models. The three-parameter models were reduced to two-parameter models by calculating the deadwater fraction based on the internal volume of the vessel and the void volume of the solids region. Thus, only the experiments performed with solids contained in the calciner were analyzed by these multiparameter models. In each case, model parameters were obtained from the moments of the experimental concentration-time curve.

### Experimental Data and Results

A summary of experimental conditions with some calculated results is shown in Table 1. Model parameters $\mathcal{D}$ and $K$ were calculated from the second and third moments of the concentration-time curve with the aid of a computer program. A trial and error approach was employed for calculating $\mathcal{D}$ and $K$ from Eqs. 11 and 12 because these equations could not be written explicit in these parameters. Those cases where the code failed to find the zeros of Eqs. 11 and 12 are indicated in the table, and the best estimate is listed. Poor convergence is characterized by large values of $K$, because the tail of the experimental distribution decayed rapidly. However, these points should not be considered in any correlation of the results.

The dispersion numbers computed by the open and closed vessel models compare favorably for all cases, which is not surprising since the dispersion numbers are small. The dispersion number for the closed vessel model is somewhat larger than for the open vessel model. Dispersion numbers computed for the new model are usually smaller. Examination of the results shows that when no solids are present the dispersion number is a monotonically increasing function of flow rate and increases with decreased rotational speed. Presumably, at higher rotational speed, the flow is stabilized. However, when solids are in the drum, the dispersion numbers decrease with increased flow rate up to approximately $0.50 \times 10^{-3}$ $m^3/s$ and then increase with flow rate. Furthermore, at low flow rates, the dispersion numbers appear to increase with increased rotational speeds; and at high flow rates, the numbers decrease with increased rotational speed. Figure 6 depicts these effects graphically for a 5.1% solids holdup. It appears that a change in the controlling mixing mechanism is occurring. It can be speculated that at high gas flow rates, convective forces dominate; whereas at low flow rates, the solids cascading through the gas phase is the major mixing force. Remember that dispersion can result from either profiles in the (time) average velocity and random eddy motions generated by gas alone or cascading solids. The relative magnitudes of these two mechanisms can also change with gas flow rate, solid loadings, and rotational rate. In examining the results, increasing holdup appears to decrease the dispersion number.

The parameters from the new model, dispersive flow with interactive deadwater, may be compared with the parameters of the tanks-in-series with interactive deadwater model. Spencer (1981a) has shown that $\mathcal{D}$ and $\mathcal{D}_e$ compare to within 20%; $\mathcal{D}_e$ is smaller. Values of $K$ and $K_e$ compare less favorably. The method of analysis

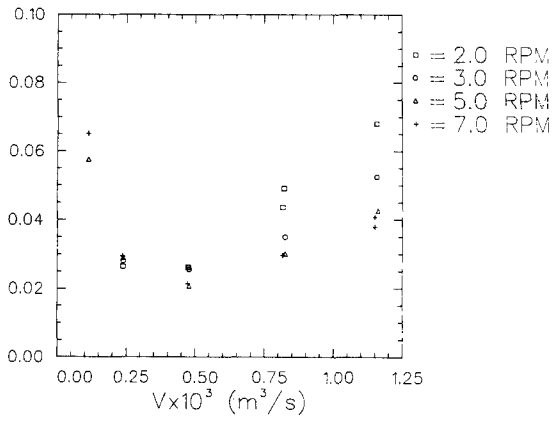


**Figure 6. Dispersion number from new model at 5.1% solids holdup.**

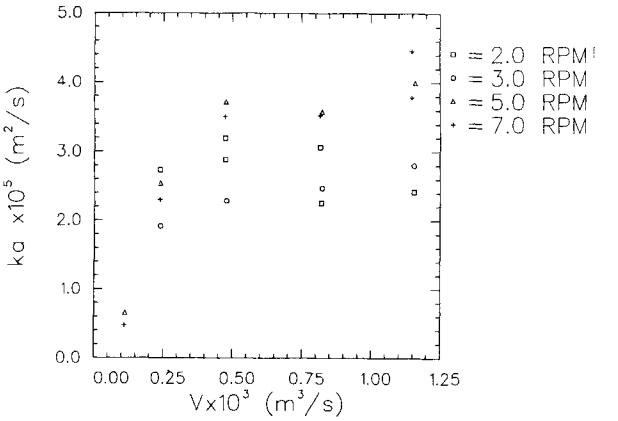


**Figure 7. Interchange rate from new model at 5.1% holdup.**

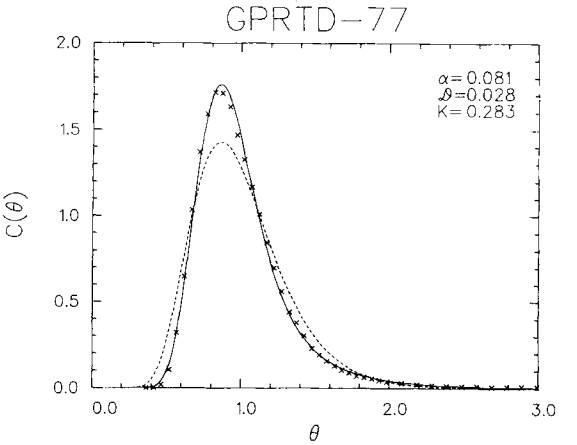


**Figure 8. Comparison of data (crosses) with new model (solid line) and ordinary dispersion model, $\mathcal{D}$ = 0.051 (dashed line), for run GPRTD-77.**

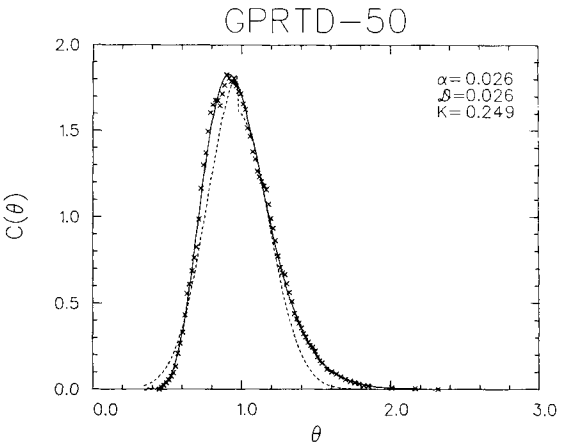


**Figure 9. Comparison of data (crosses) with new model (solid line) and tanks-in-series with deadwater model, N = 21.42 and P/V = 0.00709 (dashed line), for run GPRTD-50.**

results in an interchange factor, $K = kaL/V$. If $V$ dominates the character of $K$, any correlation of $K$ with $V$ is tantamount to plotting $V$ vs. $1/V$. It is, therefore, desirable to extract an interchange rate as follows:

$$ka = \frac{kaL}{V}\left(\frac{V}{L}\right) = K\left(\frac{V}{L}\right). \quad (28)$$

The term, $k$, is not isolated because the term, $a$, could also be a function of rotational speed (i.e., the simple chord length, a, as shown in Figure 1 may not adequately represent the interfacial area between the bulk gas and the deadwater regions). As shown in Figure 7, the interchange rate initially arises with increased flow rate but quickly levels until there is practically no further change with increasing flow rate. The interchange rate increases with rotational speed; this is particularly noticeable at the higher flow rates. Data obtained at a 15.3% solids holdup are scattered and do not show this trend as well. However, the interchange rates do appear to increase with an increase in holdup. The same observations can be drawn from calculated values of the equivalent variables obtained from the tanks-in-series with deadwater model.

### Sensitivity of Model to Errors in Data

Data from two runs were altered synthetically to simulate an error in the zero line of the concentration data. An error equivalent to 2.0% of full instrument scale was either added to or subtracted from the concentration data and the resulting data were reanalyzed. A 2% shift in the data can make a threefold change in the calculated interchange factor and about a twofold change in the dispersion number. The dispersion number was affected in like manner in the ordinary dispersion models. Thus, the results are highly sensitive to errors in the data, and this is a possible cause for the scatter in the results. Such sensitivity is probably an artifact of computing model parameters by the method of moments. Clements (1969) establishes that moments methods weight data points on the distribution unevenly. However, the moments establish an unbiased basis for comparing different models.

### Experimental Data vs. Models

The new dispersion with interactive deadwater model is compared to the data and to two previous models in Figures 8 and 9. When the tail of the distribution is long, indicating a significant effect by the stagnant zone, the new model describes the data considerably better than the usual dispersion model as shown in Figure 8. The tanks-in-series with interactive deadwater model should describe the data as well as the current model. However, since the equations for the $C$ curve for that model were derived by dropping "insignificant" terms in the transfer function, this is not the case as shown in Figure 9. Fitting the decaying exponential part of the solution to the tail of the distribution would yield a better fit to the data in that region. However, the decay constant and thus the exchange rate, would be much smaller than the exchange rates given by the moments of either model. Further, there is the problem of deciding where the tail begins.

## CLOSING REMARKS

The resulting values for axial dispersion coefficients and exchange factors are left in tabular form. No attempt was made to develop either mechanistic or empirical equations to correlate the results. It seemed inappropriate to correlate the data with an equation at this time. In the meantime, the data themselves should prove useful since they give approximate, albeit uncertain, values for $\mathcal{D}$ and $K$ over a range of conditions. Sound mechanistic theories that explain and/or predict how $\mathcal{D}$ and $K$ behave should be developed. Additional data should be obtained from different size calciners, and effects of temperature gradients should be investigated.

## ACKNOWLEDGMENTS

This work was performed in the Fuel Recycle Division of the Oak Ridge National Laboratory under the auspices of the Consolidated Fuel Reprocessing Program and was sponsored by the Office of Nuclear Fuel Cycle, U.S. Department of Energy, under Contract W-7405-eng-26 with Union Carbide Corp.

## NOTATION

$A$ = total cross-sectional area occupied by fluid, m$^2$

$a$ = chord length or length of interface at a cross section, m
$C$ = concentration in free stream, kg/m$^3$
$C_d$ = concentration in deadwater region, kg/m$^3$
$C_{in}$ = inlet concentration, kg/m$^3$
$C(\theta)$ = effluent concentration as a function of dimensionless time
$C_o$ = concentration at a prevailing steady state, kg/m$^3$
$C_{out}$ = outlet concentration, kg/m$^3$
$\mathcal{D}$ = dispersion number, $D/\bar{u}L$, dimensionless
$\mathcal{D}_e$ = equivalent dispersion number computed from tanks in series model
$D$ = dispersion coefficient, m$^2$/s
$d$ = inside diameter of calciner drum, m, or ordinary differential operator
$E$ = defined by Eq. 9
$e$ = 2.71828182845904524
$K$ = interchange factor, $kaL/V$, dimensionless
$K_e$ = equivalent interchange factor computed from tanks in series model
$k$ = interchange rate between free stream and deadwater stream, m/s
$L$ = length of calciner drum, m
$N$ = number of equal sized tanks
$n$ = integer counter
$p$ = volumetric flow rate of fluid through deadwater region, m$^3$/s
$r$ = inside radius of tube, m
$S_n^+$ = defined by Eq. 14
$S_n^-$ = defined by Eq. 15
$s$ = variable in Laplace transformed domain
$t$ = time, s
$\bar{t}$ = mean time or first moment, s
$U$ or $U(cs)$ = defined by Eq. 8
$\bar{u}$ = mean velocity, m/s
$V$ = volumetric flow rate, m$^3$/s
$x$ = variable measuring length, m
$z$ = dimensionless length, $x/L$

### Greek Letters

$\alpha$ = fraction of vessel composed of deadwater region
$\gamma^3$ = skewness factor or third moment, s$^3$
$\gamma_\theta^3$ = normalized skewness factor or third moment, dimensionless
$\Delta$ = change
$\partial$ = partial differential operator
$\epsilon$ = defined implicitly by Eq. 19
$\epsilon_n$ = nth root of Eq. 19
$\theta$ = dimensionless time, $t/\bar{t}$
$\bar{\theta}$ = mean dimensionless time
$\sigma^2$ = variance or second moment, s$^2$
$\sigma_\theta^2$ = normalized variance or second moment
$\phi_n$ = defined by Eq. 18
$\Omega_n^+$ = defined by Eq. 16
$\Omega_n^-$ = defined by Eq. 17

## LITERATURE CITED


Clements, Jr., W. C., "A Note on Determinations of the Parameters of the Longitudinal Dispersion Model from Experimental Data," *Chem. Eng. Sci.*, **24**, 957 (1969).

Danckwerts, P. V., "Continuous Flow Systems," *Chem. Eng. Sci.*, **2**, 1 (1953).

Levich, V. G., V. S. Markin, and Yu. A. Chismadzhev, "On Hydrodynamic Mixing in a Model of Porous Medium With Stagnant Zones," *Chem. Eng. Sci.*, **22**, 1357 (1967).

Mickley, H. S., T. K. Sherwood, and C. E. Reed, *Applied Mathematics in Chemical Engineering*, 2nd ed., 289, McGraw-Hill Book Co., New York (1957).

Spencer, B. B., "Gas Phase Dispersion in a Small Rotary Kiln," M.S. Thesis, University of Tennessee, Knoxville, TN (1981a).

Spencer, B. B., *Gas Phase Dispersion in a Small Rotary Kiln*, ORNL-5733, Oak Ridge National Laboratory, Oak Ridge, TN (1981b).

Van Deemter, J. J., F. J. Zuiderwig, and A. Klinkenburg, "Longitudinal Diffusion and Resistance to Mass Transfer as Causes of Nonideality in Chromatography," *Chem. Eng. Sci.*, **5**, 271 (1956).

Van der Laan, E. Th., "Notes on the Diffusion-Type Model for the Longitudinal Mixing in Flow," *Chem. Eng. Sci.*, **7**, 187 (1957).

Wehner, J. F., and R. H. Wilhelm, "Boundary Conditions of Flow Reactor," *Chem. Eng. Sci.*, **6**, 89 (1956).

Wen, C. Y., and L. T. Fan, *Models for Flow Systems and Chemical Reactors*, 113 and 468, Marcel Dekker, Inc., New York (1975).

Wylie, C. R., *Advanced Engineering Mathematics*, 4th ed., 803, McGraw-Hill Book Co., New York (1975).



*Manuscript received September 14, 1981; revision received April 29, and accepted May 13, 1982.*